Technique for Predicting Longitudinal Pilot-Induced Oscillations

R. A. Hess* and R. M. Kalteis†
University of California, Davis, Davis, California 95616

A technique for predicting the susceptibility of an aircraft to longitudinal pilot-induced oscillations (PIOs) is proposed. The technique employs the optimal control model (OCM) of the human pilot formulated for pitch attitude command tracking tasks. The criterion is very simple and is based solely on the characteristics of the pilot/vehicle open-loop transfer function as predicted by the OCM. The criterion has its genesis in the results of a previous study using the OCM in pitch attitude tracking tasks and was evaluated here using results from flight tests of 25 configurations flown on the NT-33 variable stability aircraft and three additional configurations from flight tests of a high-performance aircraft. Only the index of performance weighting coefficients in the OCM are considered as model variables, and a technique for generating these coefficients is reviewed.

Introduction

AN analytical technique that can correctly assess an aircraft's susceptibility to pilot-induced oscillations (PIOs) early in the design stage would be a very useful tool for the flight control/handling qualities engineer. The PIO theory and resulting prediction technique developed by Smith,[1] and evaluated by Twisdale and Kirsten[2] and more recently and extensively by Bjorkman et al.,[3] has been quite successful in predicting PIOs. Nonetheless, Smith's technique would appear to require experience in selecting appropriate models of piloted control of pitch attitude, not always a trivial task. The authors of Ref. 3 state, "Smith's theory can accurately predict both PIO tendencies and frequencies when used with a properly parameterized pilot model. This need for an accurate pilot model is a major drawback to Smith's theory." It is one of the objectives of the research reported herein, to present a PIO prediction method that, while still requiring an accurate pilot model, provides a formal procedure for its generation.

In what follows, the optimal control model (OCM) of the human pilot will be briefly described first,[4] with emphasis on the method for obtaining the index of performance weighting coefficients. Next, qualitative correlations between OCM-generated pilot/vehicle pitch attitude characteristics and aircraft PIO susceptibility will be reviewed.[5] A simple criterion for PIO susceptibility will then be developed and its validity investigated using results from flight tests.[2,3,6] Finally, concluding remarks summarize the limitations of the proposed technique.

Optimal Control Model of the Human Pilot

The OCM of the human pilot is based on the hypothesis that with limitations and in well-defined control tasks, the human pilot can be described in terms of the operation of a linear optimal estimator and regulator.[4] For the single-axis tasks to be discussed here, the dynamics of the regulator part of the OCM formulation are the most important. A brief review of optimal regulator design will introduce the authors' technique for selection of the all-important OCM index-of-performance weighting coefficients for single-axis attitude control tasks. This technique relies only on the transfer function of the vehicle's attitude dynamics, including the flight-control system.

Consider Fig. 1, which represents a single-axis, attitude control task. In this task, the pilot is assumed to generate a control input $\delta(t)$, which, in terms of the OCM, is defined as the product of a feedback gain matrix and the system state vector. This $\delta(t)$ minimizes a weighted sum of mean-square tracking error and control rate given by the index of performance

$$J = E\left\{\lim_{\chi\to\infty}\frac{1}{2\chi}\int_{-\chi}^{\chi}[\theta_e^2(t)/\theta_M^2 + \dot{\delta}^2(t)/\dot{\delta}_M^2]\,dt\right\} \tag{1}$$

The weighting coefficients in Eq. (1) have been expressed as inverses of the square of "maximum allowable" deviations of the error and control rate.

A technique for choosing these maximum allowable deviations so as to generate a model of the human pilot was introduced in Ref. 5 and will be summarized here. An arbitrary maximum allowable deviation $\dot{\theta}_M$ is assigned to the attitude error rate $\dot{\theta}_e(t)$. Now an "effective time constant" T is introduced to define the maximum allowable deviations of the integral and derivatives of $\dot{\theta}_M$, as

$$\begin{aligned}
&\theta_M = \dot{\theta}_M T\\
&\dot{\theta}_M = \text{specified but arbitrary}\\
&\ddot{\theta}_M = \dot{\theta}_M/T\\
&\dddot{\theta}_M = \ddot{\theta}_M/T = \dot{\theta}_M/T^2\\
&\quad\vdots
\end{aligned} \tag{2}$$

In a similar manner, one can write

$$\begin{aligned}
&\delta_M = \dot{\delta}_M T\\
&\dot{\delta}_M = \text{to be selected}\\
&\ddot{\delta}_M = \dot{\delta}_M/T\\
&\dddot{\delta}_M = \ddot{\delta}_M/T = \dot{\delta}_M/T^2\\
&\quad\vdots
\end{aligned} \tag{3}$$

The value of $\dot{\delta}_M$ is not arbitrary, however, but is found using Eqs. (2) and (3) and the vehicle dynamics as follows. Consider the following general transfer function representation of

Received Dec. 19, 1989; revision received Oct. 15, 1989.

*Professor, Division of Aeronautical Science and Engineering, Department of Mechanical Engineering. Associate Fellow AIAA.

†Graduate Student. Student Member AIAA.

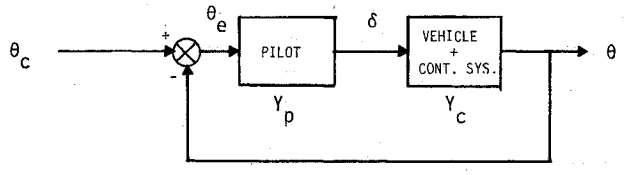

Fig. 1 Pilot/vehicle system for a single-axis attitude control task.

a vehicle's pitch attitude dynamics, including the control system

$$\frac{\theta}{\delta}(s) = K\frac{s^{n-1} + a_{n-2}s^{n-2} + \cdots + a_1 s + a_0}{s^n + b_{n-1}s^{n-1} + \cdots + b_1 s + b_0} \tag{4}$$

By considering the differential equation between $\theta(t)$ and $\delta(t)$ and replacing each derivative by its maximum allowable deviation as determined from Eqs. (2) and (3), the following relation can be obtained:

$$\dot{\delta}_M = \frac{1/T^{n-1} + |b_{n-1}|/T^{n-2} + \cdots + |b_1| + |b_0|T}{K(1/T^{n-2} + |a_{n-2}|/T^{n-3} + \cdots + |a_1| + |a_0|T)} \cdot \dot{\theta}_M \tag{5}$$

The introduction of absolute values in Eq. (5) prevents singularities from occurring in the definition of $\dot{\delta}_M/\dot{\theta}_M$. With the introduction of Eq. (5), the selection of the relative weighting between attitude error and control rate becomes synonymous with selection of the effective time constant T.

The utility of introducing the time constant T in the OCM technique can be demonstrated by considering the optimal regulator designs associated with four "stereotype" vehicle dynamics given by $Y_c = 1$, $1/s$, $1/s^2$, and $1/[s(s-1)]$. These represent, in order, attitude, rate acceleration, and second-order divergent vehicle dynamics. Table 1 shows the results of applying the effective time constant method to the selection of $\dot{\delta}_M$ and θ_M to be used in the index of performance defined in Eq. (1). Here ω_B represents the bandwidth of θ/θ_c, defined as the magnitude of that closed-loop pole closest to the frequency where $|\theta/\theta_c|$ is 6 dB below its zero frequency value. The point to be noted from Table 1 is that by keeping T constant for the different vehicle dynamics, the optimal regulator design has produced nearly constant values for ω_B, while the ratio of index of performance weighting coefficients determined from Eq. (5) and employed in Eq. (1) has varied by a factor of 900. Thus, as defined here, the effective time constant T appears to be directly related to the most fundamental characteristic of the optimal closed-loop regulator design, namely, its bandwidth.

The analysis of a variety of single-axis manual control tasks using the complete OCM (regulator and estimator), suggests the following approximate relationship for choosing T, (Ref. 5)

$$T = 0.65(\tau_P) \text{ s} \tag{6}$$

where τ_P is the value for the human pilot time delay, nominally 0.2 s in the OCM. Equation (6) has proved most useful when the dynamics of the vehicle are of third order or less with pole/zero magnitudes less than 10 rad/s. The OCM can, however, produce unrealistic pilot models in certain single-axis tracking applications in which the vehicle possesses higher-order, high-frequency dynamics. In these cases one often finds the OCM predicting unstable pilot compensation, e.g., a pair of complex poles in the right half plane (RHP). This phenomenon occurs when index of performance weighting coefficients have been chosen with Eq. (6) or as those that yield "neuromotor" time constants on the order of 0.1 s, an acceptable procedure in most applications.[7] The problem here is that the OCM is exploiting its precise knowledge of the higher-order, high-frequency vehicle dynamics. One way to circumvent this difficulty is to use a lower-order equivalent system representation for the vehicle dynamics wherein the higher-order, high-frequency dynamics are subsumed into an effective time delay τ_D. Equation (1) is then rewritten as

$$T = 0.65(\tau_P + \tau_D) \text{ s} \tag{7}$$

Although the actual vehicle dynamics are still used in the OCM analysis, the effective time constant T and index of performance weighting coefficients are selected using the equivalent system and Eq. (7). In this study, as in Ref. 5, the equivalent system is defined when the vehicle attitude dynamics, including control system, are fit to the transfer function

$$\frac{\theta}{\delta} = \frac{K_\theta(T_L s + 1)e^{-\tau_D s}}{[s^2/\omega_n^2 + (2\zeta_n/\omega_n)s + 1]} \tag{8}$$

over the frequency range $0.1 < \omega < 20$ rad/s.

The remainder of the OCM parameters are set to nominal values in this study. Pitch attitude error and its time derivative are the variables assumed to be perceived by the pilot. Observation noise-signal ratios for each of these variables are -20 dB and the motor noise-signal ratio is -40 dB. No optimization of attention allocation between error and error rate is considered in the model.[8] The pilot time delay τ_p is set to 0.2 s. Finally, since the OCM requires that the command input be modeled as white noise passed through a shaping filter, the tasks studied here all use a pitch attitude *command* θ_c modeled as white noise passed through a second-order filter $1/[s+1]^2$. The magnitude of the command input is of no consequence in this analysis. It is imperative to point out that since the PIO criterion to be derived will be evaluated using the command signal just described, changing the characteristics of this signal can affect the results of an analysis. In particular, increasing the command signal bandwidth beyond 1 rad/s may induce crossover frequency regression that is not related to the PIO susceptibility of the aircraft, itself. The code used to generate the OCM in this study is described in Ref. 9.

Pilot-Induced Oscillation Criterion

The criterion for predicting an aircraft's susceptibility to longitudinal PIOs is based entirely on the characteristics of

Table 1 Optimal regulator characteristics for stereotype vehicle dynamics

Y_c	T, s	$\frac{\dot{\delta}_M}{\theta_M}$, 1/s	$\frac{\theta}{\theta_c} = \frac{Y_p Y_c}{1 + Y_p Y_c}$	ω_B, rad/s
1	0.2	5.0	$\frac{5}{(s+5)}$	5.0
$1/s$	0.2	25.0	$\frac{25}{(s^2+7.07s+25)}$	5.0
$1/s^2$	0.2	125.0	$\frac{5(s+2.5)}{(s+5)(s^2+5s+25)}$	5.0
$1/[s(s-1)]$	0.2	150.0	$\frac{68.2(s+2.19)}{(s+5.35)(s^2+5.33s+28)}$	5.35

DESCRIPTION	NUMERICAL RATING
NO TENDENCY FOR PILOT TO INDUCE UNDESIRABLE MOTIONS.	1
UNDESIRABLE MOTIONS TEND TO OCCUR WHEN PILOT INITIATES ABRUPT MANEUVERS OR ATTEMPTS TIGHT CONTROL. THESE MOTIONS CAN BE PREVENTED OR ELIMINATED BY PILOT TECHNIQUE.	2
UNDESIRABLE MOTIONS EASILY INDUCED WHEN PILOT INITIATES ABRUPT MANEUVERS OR ATTEMPTS TIGHT CONTROL. THESE MOTIONS CAN BE PREVENTED OR ELIMINATED BUT ONLY AT SACRIFICE TO TASK PERFORMANCE OR THROUGH CONSIDERABLE PILOT ATTENTION AND EFFORT.	3
OSCILLATIONS TEND TO DEVELOP WHEN PILOT INITIATES ABRUPT MANEUVERS OR ATTEMPTS TIGHT CONTROL. PILOT MUST REDUCE GAIN OR ABANDON TASK TO RECOVER.	4
DIVERGENT OSCILLATIONS TEND TO DEVELOP WHEN PILOT INITIATES ABRUPT MANEUVERS OR ATTEMPTS TIGHT CONTROL. PILOT MUST OPEN LOOP BY RELEASING OR FREEZING THE STICK.	5
DISTURBANCE OR NORMAL PILOT CONTROL MAY CAUSE DIVERGENT OSCILLATION. PILOT MUST OPEN CONTROL LOOP BY RELEASING OR FREEZING THE STICK.	6

Fig. 2 PIOR scale.

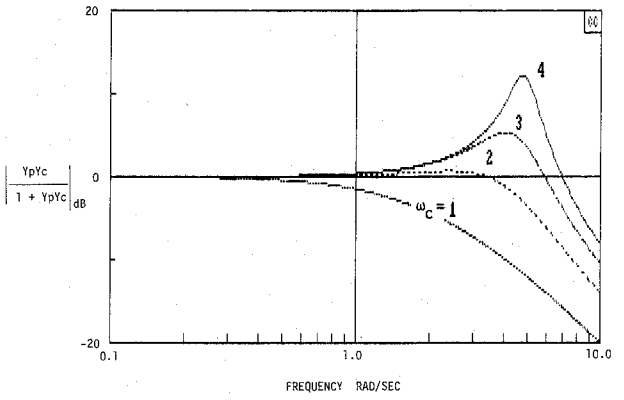

Fig. 3 Closed-loop amplitude characteristics of system of Fig. 1; Y_pY_c of Eq. (9) with $\tau_e = 0.3$ s.

the pilot/vehicle open-loop transfer function (Y_pY_c in Fig. 1) obtained from application of the OCM when parameterized as just described. It should be emphasized at the outset that the OCM itself will never exhibit PIOs, i.e., it will always produce a stable closed-loop system. However, in using the OCM to model the pilot control of pitch attitude for a number of different flight-test configurations in Ref. 5, the shape of the amplitude portion of the Bode diagram for vehicles that were judged to be PIO prone in flight test were distinctly different than those that were not. Specifically, as compared to the configurations that were not determined to be PIO prone in flight, $|Y_pY_c(j\omega)|$ for the PIO prone configurations exhibited considerably lower crossover frequencies and $|Y_pY_c(j\omega)|$ vs exhibited slopes more shallow than the desirable -20 dB/decade below the crossover frequency. The manner in which these characteristics could lead to the development of a PIO was outlined in Ref. 5 and will be discussed later.

These results led to a very simple PIO criterion of Ref. 5 that required only a minimum crossover frequency (1.5–2 rad/s) to be predicted by a pilot/vehicle analysis to exonerate a vehicle from PIO tendencies. The aforementioned reduction in slope of the Y_pY_c amplitude curve was not included in the criterion. Although Ref. 5 stated that any "valid" pilot/vehicle model could be used in the PIO analysis, in retrospect, it would have been more advisable to limit the criterion to modeling results obtained with the OCM as parameterized in that study. This more cautious approach will be adopted here.

Most of the PIO-prone configurations analyzed in Ref. 5 exhibited very strong PIO tendencies in flight. It is very desirable to be able to identify vehicle configurations that exhibit weaker tendencies but nonetheless would be considered to be PIO prone by pilots. This leads naturally to the pilot-induced-oscillation rating scale (PIOR) shown in Fig. 2 and to the adoption of the same PIO standard as used in Ref. 3. Namely, a vehicle is considered PIO prone if it received a PIOR of 2 or greater in flight tests.

The adoption of this rigorous definition of PIO proneness demands a criterion more precise than the rather loose 1.5–2.0 rad/s crossover frequency limit suggested in Ref. 5. The problem of formulating this criterion was approached by first identifying a specific lower limit on the crossover frequency and then by incorporating a requirement on the amplitude characteristics of $|Y_pY_c(j\omega)|$ at frequencies below crossover. The revised criterion thus reflects the $|Y_pY_c(j\omega)|$ slope reduction reported in Ref. 5 and linked in that study to the development of PIOs. The revised criterion is developed by heuristic arguments and the results of Ref. 5 and then evaluated by appealing to the flight-test results described in Refs. 2, 3, and 6.

Minimum Crossover Frequency

Consider a crossover model[10] for pitch attitude tracking. The model states that, around crossover, Y_pY_c can be approximated as

$$Y_pY_c = [\omega_c e^{-\tau_e s}]/s \tag{9}$$

where τ_e is an effective time delay in the approximate range 0.25–0.35 s. Figure 3 shows the amplitude portions of the Bode diagrams for the closed-loop pilot/vehicle pitch attitude

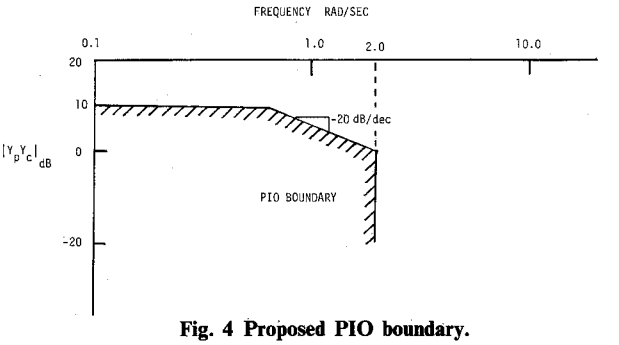

Fig. 4 Proposed PIO boundary.

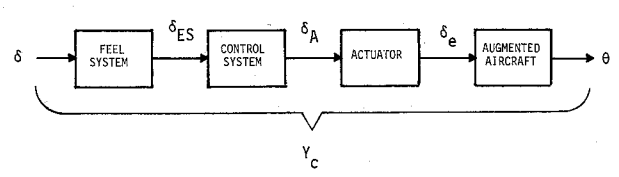

$$\frac{\delta_{ES}}{\delta} = \frac{K_{FS}}{s^2/26^2 + 2(.6)s/26 + 1} \qquad \frac{\theta}{\delta_e} = K_\theta \frac{(1.4s + 1)}{s[s^2/\omega_{sp}^2 + 2(\tau_{sp})s/\omega_{sp} + 1]}$$

$$\frac{\delta_A}{\delta_{ES}} = \text{SEE TABLES} \qquad \frac{\delta_e}{\delta_A} = \frac{K_A}{s^2/75^2 + 2(.7)s/75 + 1}$$

Fig. 5 Vehicle and control system dynamics for configurations from Refs. 3 and 6.

Table 2 Control system definitions

First-order lag	$\frac{1}{\tau_2 s + 1}$
First-order lead/lag	$\frac{\tau_1 s + 1}{\tau_2 s + 1}$
Second-order lag	$\frac{1}{s^2/\omega_3^2 + 2(\zeta_3)s/\omega_3 + 1}$
Fourth-order lag	$\frac{1}{[s^2/\omega_3^2 + 2(\zeta_3)s/\omega_3 + 1][s^2/\omega_4^2 + 2(\zeta_4)s/\omega_4 + 1]}$
G_1	$\frac{(0.5s + 1)(0.43s + 1)}{(0.2s + 1)(1.1s + 1)[s^2/4^2 + 2(0.7)s/4 + 1]}$
G_2	$\frac{(0.5s + 1)(0.43s + 1)(0.06s + 1)}{(0.2s + 1)(0.1s + 1)(1.1s + 1)}$

Table 3 Configuration definitions; LAHOS data

	Aircraft	Control system			
Configuration	ω_{sp}/ζ_{sp} rad/s/–	τ_1 s	τ_2 s	ω_3/ζ_3 rad/s/–	ω_4/ζ_4 rad/s/–
1-C	1.0/0.74	0.2	0.1	—	—
2-A	2.3/0.57	0.4	0.1	—	—
2-1		—	—	—	—
3-C	2.2/0.25	0.2	0.1	—	—
4-4	2.0/1.06	—	0.5	—	—
4-10		—	—	4/0.7	—
5-3	3.9/0.54	—	0.25	—	—

Table 4 Configuration definitions; HAVE PIO data

	Aircraft	Control system			
Configuration	ω_{sp}/ζ_{sp} rad/s/–	τ_1 s	τ_2 s	ω_3/ζ_3 rad/s/–	ω_4/ζ_4 rad/s/–
H2-B	2.4/0.64	0.3	0.1	—	—
1		—	—	—	—
5		—	1.0	—	—
7		—	—	12/0.7	—
8		—	—	9/0.7	—
H3-D	4.1/1.0	0.05	0.1	—	—
1		—	—	—	—
3		—	—	—	—
6		—	—	16/0.7	—
8		—	—	9/0.7	—
12		—	—	2/0.7	—
13		—	—	3/0.7	—
H4-1	3.0/0.74	—	—	—	—
2		—	0.1	—	—
H5-1	1.7/0.68	—	—	—	—
9		—	—	6/0.7	—
10		—	—	4/0.7	—
11		—	—	16/0.93	16/0.38

systems when the Y_pY_c of Eq. (9) is used with $\tau_e = 0.3$ s and with $\omega_c = 1$, 2, 3, and 4 rad/s. Note that, with $\omega_c = 2$ rad/s, the system is slightly underdamped ($\zeta = 0.57$). For crossover frequencies below 2.0 rad/s, however, closed-loop responses to commanded attitude changes would be comparatively sluggish. This sluggishness may not be apparent to the pilot in the early part of a landing approach where task demands are not severe. However, it almost certainly would be apparent in the more critical landing flare and touchdown where precise attitude control is a must. Here, the sluggish vehicle behavior would be likely to induce an abrupt "gain" increase on the part of the pilot with the inevitable consequences of reduced gain margin and oscillatory vehicle behavior. This is particularly true if the $|Y_pY_c(j\omega)|$ slope reduction just described is also present. A review of pilot comments in Ref. 6 supports this conjecture. Quoting from Ref. 6, "The more stringent flare and touchdown task exposes the 'flying qualities cliffs' hidden in PIO prone aircraft." Thus, on the basis of this very simple heuristic argument, it would appear that 2.0 rad/s represents a reasonable estimate for the lower limit on the crossover frequency to be used in the PIO criterion.

Slope Reduction

Slope reduction in $|Y_pY_c(j\omega)|$ at frequencies below crossover also contributes to poor closed-loop transient response and increases the sensitivity of changes in gain margin to changes in crossover frequency.[5] Based on the Bode diagrams appearing in Ref. 5, it was decided that -20 dB/decade for at least one half decade below the minimum crossover frequency should be required to ensure a low-frequency amplitude of at least 10 dB. Below this frequency, flat amplitude characteristics would be acceptable.

Optimal Control Model Pilot-Induced Oscillations

Figure 4 shows the resulting frequency domain boundary. Summarizing, if any portion of $|Y_pY_c(j\omega)|$ obtained from the OCM as parameterized in the preceding discussion touches or crosses the boundary of Fig. 4, the resulting vehicle configuration will be considered to be PIO prone, i.e., it will be assumed to warrant a PIOR of 2.0 or greater. Next, experimental results from Refs. 2, 3, and 6 will be used to evaluate and, if necessary, refine this criterion.

Criterion Evaluation

Configurations Analyzed

Figure 5 shows the vehicle and control system pitch attitude dynamics for the experimental configurations flight tested in Refs. 6 (referred to as the LAHOS data) and 3 (referred to as the HAVE PIO data), with Table 2 defining pertinent control system dynamics. Tables 3 and 4 complete the configuration descriptions from these two references. Table 5 gives the vehicle/control system attitude dynamics for the three configurations from Ref. 2, referred to there and here as simply a high-performance aircraft. Table 6 lists the effective time constant values and weighting coefficients resulting from the application of Eqs. (7) and (8) to the open-loop pitch attitude dynamics of vehicle-plus control system for all the configurations. The weighting coefficients listed in Table 6 were obtained from the equivalent system fits shown in Table 7. As Eq. (5) indicates, the PIO prediction method will not be sensitive to control command gain K. This is because changes in K result in reciprocal changes in $\dot{\delta}_M$, and the predicted Y_pY_c will remain invariant.

Although 42 configurations were flight tested in Ref. 6, just seven were used in the evaluation here. These were selected on the basis of 1) nearly equal representation of vehicles with and without PIO susceptibility as indicated by the PIOR, and whose PIO susceptibility was felt to be conclusive,[11] and 2) a representation of different control system types. All 18 configurations flight tested in Ref. 3 were evaluated. In the analysis of configurations from Refs. 3 and 6, the second-order actuator dynamics with a break frequency of 75 rad/s were neglected. The second-order feel system dynamics with a break frequency of 26 rad/s and a damping ratio of 0.6 were modeled by an effective time delay of 0.06 s. This 0.06-s value was added to the pilot's time delay in the OCM and included in Eq. (7). Table 8 lists the OCM predicted crossover frequencies and unstable frequencies. These values were obtained graphically and so are approximate. The unstable frequency is the frequency at which the phase of $Y_pY_c(j\omega)$ passes through -180 deg and does not imply susceptibility to PIOs. These unstable frequencies are, in general, poor predictors of PIO frequencies. This is not surprising since, as mentioned previously, the OCM technique is only intended to indicate PIO proneness or susceptibility and will not necessarily provide information about pilot/vehicle dynamics during a PIO itself.

Table 5 Configuration definitions; high-performance aircraft data[a]

Landing approach

$$\frac{\theta}{\delta_{ES}} = \frac{-2.33 \times 10^7(-31)(1.8)(1.5)(0.661)}{(0)(41.52)[0.778,42.21][0.567,35.59](8.852)(5.806)[0.703,1.385](0.831)} \text{ (rad/deg)}$$

Up and away

$$\frac{\theta}{\delta_{ES}} = \frac{-2.217 \times 10^7(-31)(0.588)(0.578)(1.5)}{\underbrace{(0)(40.965)[0.776,41.84][0.574,35.45](11.913)[0.753,2.290][0.989,0.608]}_{\Delta}} \text{ (rad/deg)}$$

Up and away plus display

$$\frac{x^b}{\delta_{ES}} = \frac{-1.330 \times 10^7(-31)(0.588)(0.578)(1.5)}{\Delta(2)} \text{ (--/deg)}$$

[a]Notation: Gain = a, $(s+a) = (a)$, $(s^2 + 2\zeta\omega s + \omega^2) = [\zeta,\omega]$.
[b]x = attitude cue presented to pilot on cockpit display.

Table 6 Optimal control model effective time constant and index of performance weighting coefficients

Configuration	T, s	$1/\theta^2_M$	$1/\dot{\delta}^2_M$	Configuration	T, s	$1/\theta^2_M$	$1/\dot{\delta}^2_M$
1-C	0.170	34.8	0.00183	H-3	0.217	21.2	0.0592
2-A	0.169	34.9	0.0893	H3-6	0.223	20.0	0.146
2-1	0.170	34.5	0.0237	H3-8	0.253	15.6	0.161
3-C	0.297	34.9	0.0387	H3-12	0.346	8.4	0.0636
4-4	0.257	15.1	0.107	H3-13	0.322	9.62	0.104
4-10	0.342	8.5	0.0516	H4-1	0.170	34.7	0.0445
5-3	0.237	17.8	0.130	H4-2	0.211	22.4	0.067
H2-B	0.169	34.9	0.0682	H5-1	0.170	34.7	0.00812
H2-1	0.170	34.8	0.0253	H5-9	0.316	10.0	0.0571
H2-5	0.170	34.7	0.000973	H5-10	0.370	7.3	0.0791
H2-7	0.246	16.6	0.0770	H5-11	0.278	12.9	0.0418
H2-8	0.269	13.8	0.0968	Landing	0.247	16.4	0.0115
H3-D	0.177	31.7	0.0686	Up-away	0.260	14.8	0.0140
H3-1	0.170	34.7	0.080	Up-away + Display	0.260	14.8	0.00164

Results of Criterion Evaluation

Table 9 summarizes the OCM PIO analysis and also gives the average PIORs from flight tests. Figure 6 demonstrates the variations in OCM Y_pY_c amplitude and phase characteristics that occurred in the evaluation. As the figure indicates, these correspond to configuration 2-1 from Ref. 6 (average PIOR of 1.0), configuration H3-12 from Ref. 3 (average PIOR of 4.5), and the landing configuration from Ref. 2 (no PIOR given, but a PIO experienced in flight). In the 28 configurations analyzed with the OCM and evaluated with the PIO criterion shown in Fig. 4, only four "failures" were found. These were configuration 2-A in the LAHOS study and configurations H2-B, H3-1, and H3-6 in the HAVE PIO study. These four were exonerated by the OCM analysis, but all were judged to be PIO prone in flight. As Table 9 indicates, the largest average PIOR for these four was 2.33 for configuration H3-1. It is interesting to note that Smith's method failed to indicate PIO proneness on configurations 2-A, H3-1, H3-3 and H3-6.[3] Since configurations 2A and H3-1 have the higher PIOR ratings of the failures, it is of interest to examine these cases a bit further.

In reading the pilot comments for configuration 2A, it is apparent that *high-frequency* PIOs were encountered, almost a "pitch-ratcheting." The following pilot comments are pertinent. Pilot A: "Had a fast, staircase type approach to final response...There was a high frequency hunting for the ground." Pilot B: "Get a high frequency bobble in flair...Very high frequency PIO evident in flare. Doesn't really affect task much. Annoying." Reference 3 reports that the average PIO frequency for configuration H3-1 was 10.64 rad/s, again a

Table 7 Lower-order equivalent system parameters

Configuration	K_θ	T_L, s	ω_n, rad/s	ζ_n	τ_D, s
1-C	1.0	1.82	1.0	0.87	0.00094
2-A	0.97	1.89	3.41	0.78	0.00035
2-1	1.0	1.43	2.31	0.57	0.0019
3-C	0.97	1.65	2.31	0.28	0.00042
4-4	1.0	1.04	1.43	0.76	0.136
4-10	1.0	1.04	1.77	0.73	0.266
5-3	1.0	1.25	3.18	0.54	0.105
H2-B	0.98	1.72	3.32	0.83	0.0004
H2-1	1.0	1.43	2.41	0.63	0.00087
H2-5	1.02	0.21	1.98	0.44	0.0010
H2-7	1.0	1.41	2.40	0.62	0.118
H2-8	1.0	1.39	2.38	0.60	0.154
H3-D	1.0	1.39	3.71	0.88	0.013
H3-1	1.0	1.43	4.24	0.98	0.00098
H3-3	1.0	1.33	2.79	0.80	0.0745
H3-6	1.0	1.39	4.05	0.90	0.0838
H3-12	1.0	1.32	3.61	0.78	0.129
H3-13	1.0	1.19	2.19	0.59	0.236
H4-1	1.0	1.43	3.05	0.73	0.001
H4-2	1.0	1.37	2.82	0.68	0.0649
H5-1	1.0	1.43	1.70	0.68	0.001
H5-9	1.0	1.35	1.68	0.63	0.226
H5-10	1.0	1.23	1.62	0.57	0.309
H5-11	1.0	1.43	1.71	0.68	0.168
Landing	1.0	0.55	1.96	1.0	0.180
Up-away	1.0	0.72	2.89	1.0	0.200
Up-away + Display	1.0	0.0	4.0	1.0	0.200

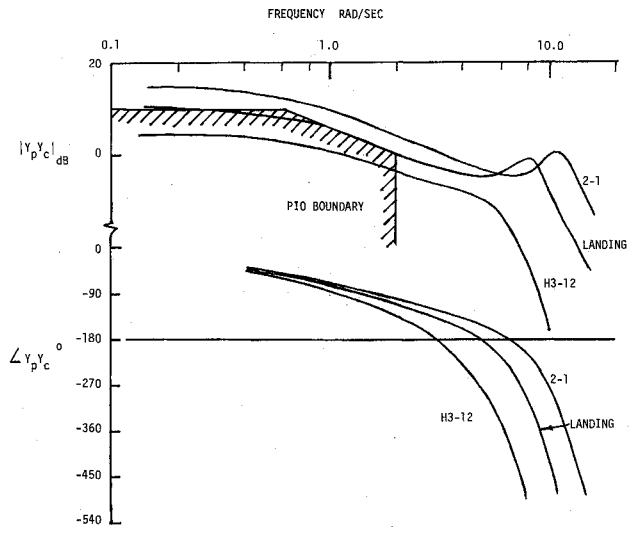

Fig. 6 Bode plots for Y_pY_c generated by the OCM for configurations 2-1 from Ref. 6, H3-12 from Ref. 3, and the landing approach from Ref. 2.

frequency typically associated with ratcheting. Indeed, one of the evaluation pilots, pilot B, reported, "Pitch movement characterized by small jerky motions, did not affect task performance." As presently formulated, the criterion proposed here will not predict such high-frequency oscillations. They appear similar to the "roll ratchet" oscillations that have occurred in roll-attitude tracking tasks with high-performance aircraft.[12] It has been suggested in the literature that these oscillations are attributable to the effects of motion cues and the characteristics of the limb/manipulator/force-feel system combination.[13,14] Work is presently underway in extending the criterion to handle these cases. The PIOs in the remaining two configurations that failed the evaluation were not high frequency in nature, and judging from pilot comments in Ref. 6 and the published PIO frequencies in Ref. 3, the configurations that were correctly identified to be PIO prone by the OCM did not experience high-frequency oscillations. Since the two remaining failures were borderline (average PIOs of 2.0), and 24 of the configurations were correctly categorized, it was felt that changes in the proposed criterion were not warranted.

Technique Summarized

The steps involved in the proposed longitudinal PIO prediction technique can now be summarized. It is assumed that

Table 8 Optimal control model crossover and unstable frequencies

Configuration	ω_c, rad/s	ω_u, rad/s	Configuration	ω_c, rad/s	ω_u, rad/s
1-C	3.0	6.0	H3-3	2.3	4.8
2-A	3.0	6.2	H3-6	2.4	5.2
2-1	2.9	6.0	H3-8	1.9	4.6
3-C	2.7	5.7	H3-12	1.1	3.2
4-4	1.7	4.0	H3-13	1.3	3.4
4-10	1.1	3.2	H4-1	3.0	6.0
5-3	2.2	4.6	H4-2	2.4	5.0
H2-B	3.1	6.0	H5-1	2.9	5.9
H2-1	3.0	6.0	H5-9	1.3	3.3
H2-5	1.9	4.2	H5-10	0.9	2.9
H2-7	1.9	4.4	H5-11	1.6	3.8
H2-8	3.0	6.0	Landing	1.9	4.2
H3-D	3.1	6.4	Up-away	1.9	4.2
H3-1	3.1	6.4	Up-away + Display	1.3	3.4

Table 9 Results of evaluation of pilot-induced oscillations criterion

Configuration	PIOR from flight (avg)	OCM PIO prone?	Configuration	PIOR from flight (avg)	OCM PIO prone?
1-C	1.0	no	H3-3	1.67	no
2-A	2.25	no	H3-6	2.0	no
2-1	1.0	no	H3-8	3.67	yes
3-C	1.25	no	H3-12	4.5	yes
4-4	2.67	yes	H3-13	4.5	yes
4-10	4.0	yes	H4-1	1.0	no
5-3	2.83	yes	H4-2	1.33	no
H2-B	2.0	no	H5-1	1.0	no
H2-1	1.0	no	H5-9	4.0	yes
H2-5	4.33	yes	H5-10	5.0	yes
H2-7	3.0	yes	H5-11	3.0	yes
H2-8	4.0	yes	Landing	N/A[a]	yes
H3-D	1.0	no	Up-away	N/A[a]	yes
H3-1	2.33	no	Up-away + Display	N/A[a]	yes

[a]No PIOR given; however, vehicle experienced PIO.

vehicle pitch attitude θ is the variable being controlled. If a display is being used involving a variable that is derived from θ (e.g., the variable x in the last configuration in Table 5), substitute that variable for θ in the following.

1) Obtain a model of the pitch attitude dynamics of the vehicle at the flight condition of interest. This model should include all control and display system dynamics.

2) Fit this model to the lower-order transfer function given by Eq. (8).

3) With $\tau_P = 0.2$ s and the τ_D from the lower-order fit, compute the effective time constant for the OCM analysis using Eq. (7).

4) Calculate the weighting coefficients to be used in the index of performance defined in Eq. (1).

5) Set up the OCM so that attitude error and error rate are the perceived variables. Set the observation noise-signal ratios to -20 dB for each of these. Use -40 dB for the motor noise signal ratio. Use a command attitude signal as white noise passed through a second-order filter $1/(s+1)^2$. The intensity of this noise is arbitrary.

6) Plot the $Y_p Y_c$ transfer function generated by the OCM and determine if the PIO boundary of Fig. 4 has been violated. If it has not, assume the vehicle is not PIO prone.

Concluding Remarks

The technique offered here for PIO prediction has not been derived from a rigorous theory for PIOs. Rather it extends and refines the modeling results of a previous study that qualitatively correlated OCM pilot/vehicle transfer functions with PIO susceptibility as determined from flight tests. The technique is appealing in that it provides a formal procedure for generating the pilot model that forms the basis of the proposed PIO criterion. The fact that the OCM is not, of itself, capable of describing the dynamics of a PIO encounter prevents the technique from being used to predict PIO frequencies with any accuracy. The technique will not, at present, predict high-frequency longitudinal PIOs or PIOs that are attributable to inappropriate command gains.

Acknowledgment

This research was performed under Grant NCC 2-490, NASA Ames Research Center, Dryden Flight Research Facility. Donald T. Berry was the contract technical manager.

References

[1]Smith, R. H., "A Theory for Longitudinal Short-Period Pilot Induced Oscillations," Air Force Flight Dynamics Lab., Wright-Patterson AFB, OH, AFFDL-TR-77-57, June 1977.

[2]Twisdale, T. R., and Kirsten, P. W., "Prediction and Occurrence of Pilot-Induced Oscillations in a Flight Test Aircraft," *Journal of Guidance, Control, and Dynamics*, Vol. 7, No. 4, 1984, pp. 410–415.

[3]Bjorkman, E. A., Silverthorn, J. T., and Calico, R. A., "Flight Test Evaluation of Techniques to Predict Longitudinal Pilot Induced Oscillations," AIAA Paper 86-2253, Aug. 1986.

[4]Kleinman, D. L., Baron, S., and Levison, W. H., "An Optimal Control Model of Human Response, Pts. I and II," *Automatica*, Vol. 6, May 1970, pp. 357–369.

[5]Hess, R. A., "Analysis of Aircraft Attitude Control Systems Prone to Pilot-Induced Oscillations," *Journal of Guidance, Control, and Dynamics*, Vol. 7, No. 1, 1984, pp. 106–112.

[6]Smith, R. E., "Effects of Control System Dynamics on Fighter Approach and Landing Handling Qualities," Vol. I, Air Force Flight Dynamics Lab., Wright-Patterson AFB, OH, AFFDL-TR-78-122, March 1978.

[7]Garg, S., and Schmidt, D. K., "Cooperative Synthesis of Control and Display Augmentation," *Journal of Guidance, Control, and Dynamics*, Vol. 12, No. 1, 1989, pp. 45–61.

[8]Curry, R. E., Kleinman, D. L., and Hoffman, W. C., "A Model for Simultaneous Monitoring and Control," *Proceedings of the 11th Annual Conference on Manual Control*, May 1975, NASA TMX-62, 464, pp. 144–150.

[9]Doyle, K. M., and Hoffman, W. C., "Pilot Modeling for Manned Simulation," Vol. II, Air Force Flight Dynamics Lab., Wright-Patterson AFB, OH, AFFDL-TR-76-24, Dec. 1976.

[10]McRuer, D. T., and Krendel, E. S., "Mathematical Models of Human Pilot Behavior," AGARDograph 188, Jan. 1974.

[11]Bjorkman, E. A., "Flight Test Evaluation of Techniques to Predict Longitudinal Pilot Induced Oscillations," Air Force Inst. of Technology, Wright-Patterson AFB, OH, AFIT/GAE/AA/86J-1, Dec. 1986.

[12]Smith, R. E., Monagan, S. J., and Bailey, R. E., "An In-Flight Investigation of Higher Order Control System Effects on the Lateral-Directional Flying Qualities of Fighter Airplanes," AIAA Paper 81-1891, 1981.

[13]Johnston, D. E., and McRuer, D. T., "Investigation of Interactions Between Limb-Manipulator Dynamics and Effective Vehicle Roll Characteristics," NASA CR-3983, May 1986.

[14]Hess, R. A., "Analyzing Manipulator and Feel System Effects in Aircraft Flight Control," *IEEE Transactions on Systems, Man, and Cybernetics* (to be published).